Heliyon 10 (2024) e32789

Contents lists available at ScienceDirect

Heliyon

journal homepage: www.cell.com/heliyon

Research article

Unlocking the therapeutic potential of Huoxiang Zhengqi San in cold and high humidity-induced diarrhea: Insights into intestinal microbiota modulation and digestive enzyme activity

Yi Wu [a], Na Deng [a], Jing Liu [a], Ying Cai [a], Xin Yi [b], Zhoujin Tan [a,*]

[a] School of Traditional Chinese Medicine, Hunan University of Chinese Medicine, Changsha, China
[b] School of Pharmacy, Hunan University of Chinese Medicine, Changsha, China

ARTICLE INFO

Keywords:
Huoxiang Zhengqi San
Diarrhea mice
Cold and high humidity stress
Intestinal microbiota
Intestinal digestive enzyme activity

ABSTRACT

Huoxiang Zhengqi San (HXZQS), a traditional Chinese herbal formula, enjoys widespread use in Chinese medicine to treat diarrhea with cold-dampness trapped spleen syndrome (CDSS), which is induced by exposure to cold and high humidity stress. This study aimed to explore its therapeutic mechanisms in mice, particularly focusing on the intestinal microbiota. Forty male SPF-grade KM mice were allocated into two groups: the normal control group (H-Cc, n = 10) and the CDSS group (H-Mc, n = 30). After modeling, H-Mc was subdivided into H-Mc (n = 15) and HXZQS treatment (H–Tc, n = 15) groups. Intestinal samples were analyzed for enzyme activity and microbiota composition. Our findings demonstrated a notable reduction in intestinal lactase activity post-HXZQS treatment ($P < 0.05$). *Lactobacillus johnsonii*, *Lactobacillus reuteri*, and *Lactobacillus murinus* emerged as the main dominant species across most groups. However, in the H-Mc group, *Clostridium sensu stricto* 1 was identified as the exclusive dominant bacteria. LEfSe analysis highlighted *Clostridiales* vadinBB60 group and *Corynebacterium* as differential bacteria in the H–Tc group, and Cyanobacteria unidentified specie in the H-Mc group. Predicted microbiota functions aligned with changes in abundance, notably in cofactors and vitamins metabolism. The collinear results of the intestinal microbiota interaction network showed that HXZQS restored cooperative interactions among rare bacteria by mitigating their mutual promotion. The HXZQS decoction effectively alleviates diarrhea with CDSS by regulating intestinal microbiota, digestive enzyme activity, and microbiota interaction. Notably, it enhances *Clostridium* vadinBB60 and suppresses Cyanobacteria unidentified specie, warranting further study.

1. Introduction

In traditional Chinese medicine (TCM), cold-dampness trapped spleen syndrome (CDSS) is a type of diarrhea that is triggered by exposure to a cold and damp environment. This can manifest in various ways, including diarrhea caused by the plateau climate or acute infantile diarrhea due to a cold environment [1]. Diarrhea induced by a cold and damp environment can also occur in modern diseases such as diarrhea-predominant irritable bowel syndrome, functional diarrhea, non-infectious diarrhea, and infectious diarrhea [2,3]. This makes diarrhea with CDSS one of the six most common syndrome-type diarrhea in Chinese medicine [4]. Similarly, it's worth noting that diarrhea induced by exposure to cold and high humidity stress is also prevalent in animal husbandry, resulting in

* Corresponding author.
E-mail address: tanzhjin@sohu.com (Z. Tan).

https://doi.org/10.1016/j.heliyon.2024.e32789
Received 17 June 2023; Received in revised form 8 June 2024; Accepted 10 June 2024
Available online 12 June 2024

considerable economic losses [5–7]. While sharing identical written characters, the term "spleen" (pronounced as "pi" in Chinese) is used in both TCM and Western medicine. Nevertheless, the interpretation of this term diverges significantly between these two medical disciplines [8]. In TCM, the concept of spleen includes some organs and their functions, which are similar but not identical to those in Western medicine, including immune, digestion, and absorption functions [9]. Additionally, the pathogenesis of diarrhea with CDSS involves external stressors originating from cold and damp environments, which impede the spleen's transportation and transformation functions. This disruption leads to diarrhea characterized by the simultaneous excretion of water, nutrients, and feces [4]. Therefore, diarrhea induced by exposure to cold and humid environmental conditions falls within the spectrum of diarrhea with CDSS.

Huoxiang Zhengqi San (HXZQS) is a classic Chinese medicine formula for treating diarrhea with CDSS that has been used effectively for thousands of years in China [10]. It consists of 13 Chinese herbal medicines including *Herba Pogostemonis*, *Folium Perillae*, *Cortex Magnoliae Officinalis*, *Radix Angelicae Dahuricae*, *Pericarpium Arecae*, *Poria*, *Rhizoma Pinelliae*, *Radix Platycodonis*, *Rhizoma Atractylodis Macrocephalae*, *Pericarpium Citri Reticulatae*, *Glycyrrhizae* Radix et Rhizoma Praeparata, *Recens* Zingiberis *Rhizoma*, and Fructus Jujubae. In TCM theory, it is believed that each disease manifesting specific pathologies and symptom patterns, while Chinese herbal medicine exhibits distinct pharmacological properties and therapeutic effects. Consequently, TCM practitioners formulate tailored herbal prescriptions to address different diseases and syndrome presentations. This underscores the personalized and holistic nature of TCM treatment, constituting one of the fundamental principles in clinical practice [11]. Following this principle, HXZQS is used for diseases with CDSS and is also effective in treating novel coronavirus pneumonia, functional dyspepsia, vomiting, and heatstroke [12,13]. In China, HXZQS is produced in various oral dosage forms, including water, pills, capsules, tablets, granules, and powders, and are widely used in various medical fields such as gastroenterology, respiratory medicine, surgery, gynecology, pediatrics, and ENT [14]. However, owing to the complex composition and multiple therapeutic targets of HXZQS, researchers find it challenging to make significant progress in studying the prescription's efficacy.

Chinese herbal medicine ingredients usually undergo transformation by intestinal microbiota upon entering the intestine, rather than being directly absorbed by the host [15]. This close relationship between Chinese herbal medicines and intestinal microbiota has two major aspects. Firstly, carbohydrates, proteins, lipids, and small non-nutritive compounds in Chinese herbal medicines are converted into active metabolites by the intestinal microbiota after entering the intestine, directly affecting the therapeutic effect of TCM. Secondly, the active metabolites can regulate the composition of intestinal microbiota, which in turn influences intestinal health [16–18]. Network pharmacology studies have shown that HXZQS, excluding *Glycyrrhizae* Radix et Rhizoma Praeparata, *Recens* Zingiberis *Rhizoma*, and Fructus Jujubae have 23 target points in the treatment of functional dyspepsia (FD), of which only 5 can directly enter the bloodstream [19]. This indicates that most of the active ingredients of the prescription may require conversion into active metabolites by intestinal microbiota to treat diseases.

The intestinal microbiota balance is vital for gut health, relying on dynamic interactions and host-related compounds. Disruptions from factors like high-fat diets, antibiotics, or environmental stress can harm gut integrity. Evaluating microbiota health involves assessing bacterial growth, diversity, and functional capacity. Ecological resilience ensures ecosystem stability post-disturbance. Internal bacterial cooperation is crucial for holistically assessing microbiota changes. Digestive enzyme activity (DEA) is essential for nutrient absorption and gut health. Understanding these processes is crucial for comprehending gut health and disease mechanisms [20]. Ecological resilience refers to an ecosystem's ability to revert to its original state after disruption [21]. Internal cooperation among intestinal bacteria is vital for maintaining ecosystem stability, providing a holistic view of microbiota changes [22]. DEA is critical for efficient nutrient digestion, preventing the accumulation of unabsorbed nutrients that can exacerbate diarrhea [23]. Carbohydrates serve as a primary energy source, with disaccharides hydrolyzed into monosaccharides by intestinal enzymes. These enzymes, derived from both the host and microbiota, include lactase, sucrase, and amylase, essential for intestinal function [24–27].

In previous studies, our research team successfully established a diarrheal mice model with CDSS [28]. Therefore, our study utilized HQZQS to treat diarrhea in mice with cold-dampness trapped spleen syndrome. Subsequently, we conducted analyses on the DEA of the intestinal mucosa and contents, as well as the diversity, structure, differential analysis, functional prediction, and cooperative dynamics of the microbial community within the intestinal contents. These comprehensive analyses were undertaken to explore the intestinal microecological mechanism of HXZQS.

2. Materials and methods

2.1. Experimental animals and housing facilities

SPF-grade KM male mice, with a weight range of 18–20 g, were housed in the Animal Center of Hunan University of Chinese Medicine under controlled conditions, including a light-dark cycle, room temperature maintained at 23 ℃-25 ℃, and a relative humidity of 47 %-53 %. The sterilized mouse growth and breeding feed and drinking water were uniformly provided by the Animal Center. The feed mainly consists of soybean meal, fish meal, bran, corn, flour, as well as sources of vitamins and minerals. The animal production license number: [SCXK (Xiang) 2019-0004], and the facility use license number: [SYXK (Xiang) 2019-0009].

2.2. Chemicals and equipment

The environmental chamber was procured from a supplier in Jiangsu, China. the vertical pressure steam sterilizer was acquired from a manufacturer in Chongqing, China. The GZX-9240MBE electric blast dryer was Sourced from a supplier based in Shanghai, China. A desktop high-speed frozen centrifuge was obtained from a distributor in Changsha, China. A constant temperature shaker incubator was purchased from a vendor in Guangzhou, China.

2- nitrophenyl-β-D-galactopyranoside was purchased from Yuanye Biotechnology Co., Ltd. (Shanghai, China), 3,5-dinitrosalicylic acid from Runcheng Biotechnology Co., Ltd. (Shanghai, China), soluble starch from Pengcai Fine Chemical Co., Ltd. (Langfang, China). O-nitrophenol (ONP) was acquired from Xiechen Import and Export Co., Ltd. (Shanghai, China). Folinol was obtained from Shanghai Xinyu Biotechnology Co., Ltd. (Shanghai, China) and carboxymethylcellulose sodium (CMC-Na) was sourced from Guangzhou Songbai Chemical Co., Ltd. (Guangzhou, China).

2.3. Preparation of Huoxiang Zhengqi San decoction

According to the textbook on Chinese herbal formulas [29], the ingredients of HXZQS were used: 90 g of *Herba Pogostemonis* from Guangdong (production batch number: 2002180142), 30 g of *Folium Perillae* from Jiangsu (production batch number: 2005280022), 60 g of *Cortex Magnoliae Officinalis* from Hunan (production batch number: 2020033001), 30 g of *Radix Angelicae Dahuricae* from Henan (production batch number: SL20060801), 30 g of *Pericarpium Arecae* from Guangxi (production batch number: 1912042), 30 g of *Poria* from Hunan (production batch number: CK20061001), 60 g of *Rhizoma Pinelliae* from Sichuan (production batch number: 20181201), 60 g of *Radix Platycodonis* from Liaoning (production batch number: CK20052003), 60 g of *Rhizoma Atractylodis Macrocephalae* from Zhejiang (production batch number: NG20062304), 60 g of *Pericarpium Citri Reticulatae* from Hunan (production batch number: HH20062301), and 75 g of *Glycyrrhizae* Radix et Rhizoma Praeparata, from Gansu (production batch number: 1907025). *Recens* Zingiberis *Rhizoma*, and Fructus Jujubae were also added to the mixture. After soaking the mixture in water for 30 min, it was decocted twice for approximately 30 min each time. The resulting solution was filtered through double-layer gauze and then concentrated in a water bath to achieve a crude drug concentration of 0.24 g/mL. Finally, the concentrate was stored in a refrigerator at 4 °C.

2.4. Animals and groups

Forty male SPF-grade KM mice were used in this study. After a three-day adaptation period, the mice were assigned randomly to two groups: a normal control group (H-Cc, n = 10) and the diarrhea with CDSS group (H-Mc, n = 30). Following successful modeling, the H-Mc group was further split into two subgroups, the H-Mc group (n = 15) and the HXZQS treatment group (H–Tc, n = 15).

2.5. Experimental design

Modeling stage: We established a mouse model exhibiting diarrhea with CDSS in accordance with established protocols. Specifically, the model group mice were exposed to an environmental chamber set at (4 ± 0.5)°C and (90 ± 2)% humidity from 8:00 to 12:00 each morning for seven consecutive days, and had unlimited access to water but no food during this period. In contrast, the H-Cc group was maintained in a standard environment with a temperature range of 23 ℃-25 ℃ and a relative humidity of 47 %-53 %, while all other conditions remained the same as those for the model group.

TCM treatment stage: After the modeling phase, the mice were further randomized into the H–Tc group and the H-Mc group. The

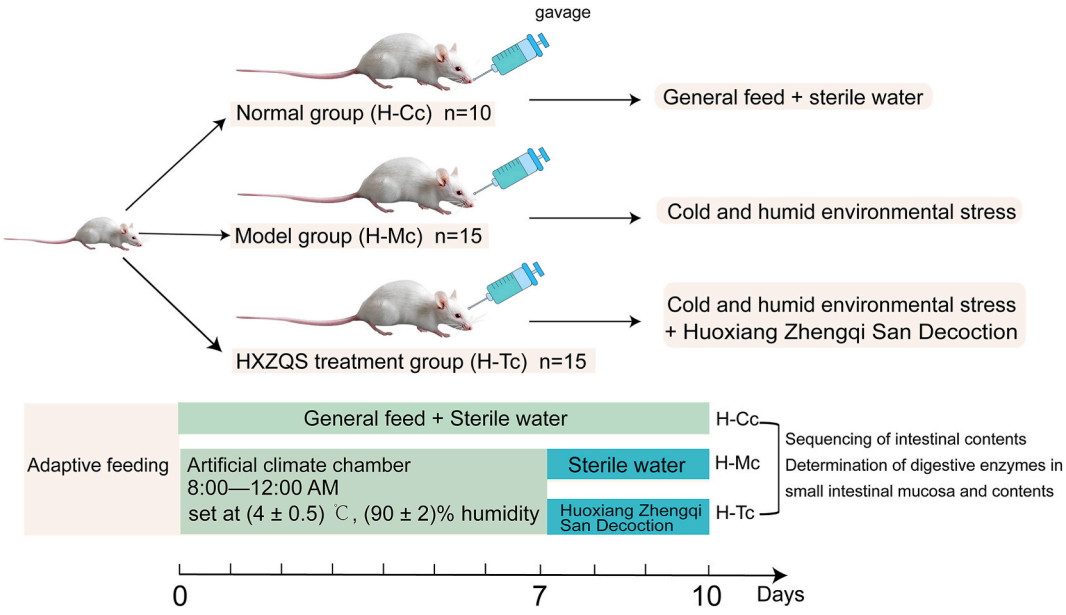

Fig. 1. Experimental design of the study. The H-Cc group represents the normal control group (n = 10), the H-Mc group represents the diarrhea with CDSS group (n = 15), and the H–Tc group represents the HXZSQ treatment group (n = 15). Likewise for subsequent groups.

H–Tc group received HXZQS decoction, while the H-Mc and H-Cc groups were given distilled water. The oral administration was given once in the morning and evening, respectively, for three consecutive days, with each mouse receiving 0.35 mL of the assigned solution per administration. A detailed experimental design is provided in Fig. 1.

2.6. Observation of general behavior and calculation of diarrhea index in mice

The behavior and characteristics of the mice was observed and recorded at a fixed time each day, including stool morphology, mental state, fur color, and anal color. At the same time each day, mice were stimulated to defecate, and fresh feces were collected separately using curved forceps onto clean filter paper for observation of fecal morphology. The degree of diarrhea in mice was graded based on the size of the wet circle on the filter paper, and the diarrhea index was calculated [30].

2.7. Small intestine contents and mucosa collection

Following the treatment, the mice were sacrificed quickly by neck dislocation. Five mice per group were selected, and small intestine samples were removed on an ultra-clean operating table. Intestinal contents were collected and marked accordingly: H-Cc 1–5, H-Mc 1–5, H–Tc 1–5. The samples were preserved at −80 °C prior to sequencing. Furthermore, we extracted the small intestinal contents/mucosa from the remaining mice in each group, recorded the weight of each sample after weighing them, and transferred them to sterile water filled with glass beads for further processing.

2.8. Detection of small intestinal content and mucosal DEA

To assess the levels of different digestive enzymes in small intestinal content and mucosa, we first prepared a crude enzyme solution using a previously established method. Thereafter, we determined lactase activity using the ONPG assay. For the detection of amylase, cellulase, and sucrase activities, we used the DNS method, and the Folin phenol method was employed for detecting protease activity. Finally, we quantified the activity levels of different digestive enzymes using a spectrophotometer. For lactase activity, 1 unit (U) was determined as the quantity of 20 mmol/L substrate decomposed within 10 min at 37 °C by 1 g of samples. Regarding amylase activity, 1 unit (U) represented the generation of 1 mg of reducing sugar per 15 min incubation at 40 °C by 1 g of samples. As for sucrase activity, 1 unit (U) signified the enzyme amount necessary to break down sucrose and yield 1 mg of glucose per min at 37 °C within 1 g of intestinal contents/mucosa. The definition of cellulase activity paralleled that of sucrase activity. In the case of protease activity, 1 unit (U) of enzyme activity was characterized by the generation of 1 mg of amino acid within a 15 min incubation period at 40 °C, catalyzed by 1 g of samples. We adhered to the referenced protocols for conducting these assays [31].

2.9. PCR amplification and illumina hiSeq sequencing

We utilized the Meiji kit (D3142-03) to extract microbial DNA from the collected samples, assessing its quantity and quality. PCR amplification of the bacterial full-length 16S rRNA gene was performed using forward primer 27F (5′-AGRGTTYGATYMTGGCTCAG-3′) and reverse primer 1492R (5′-RGYTACCTTGTTACGACTT-3′), with subsequent purification and quantification of the PCR products.

2.10. Bioinformatics analysis

To facilitate sequence assembly and de-duplication, we employed FLASH v1.2.11 software. Subsequently, the resulting high-quality sequences were clustered into operational taxonomic units (OTUs) at a 97 % threshold. OTU annotations were then compared with the Silva database to enhance taxonomic classification accuracy. The upset Venn diagrams were created between groups using R software, while the alpha diversity indices such as the Chao 1 index, ACE index [32], Shannon index [33], and Simpson index [34] were calculated using Mothur software (http://www.mothur.org/wiki/) and visualized using R package. We conducted multivariate analyses, including Principal Coordinate Analysis (PCoA) and Partial Least Squares Discriminant Analysis (PLS-DA), leveraging R packages for visualization. Our analysis encompassed generating histograms depicting microbiota abundance at both genus and species levels. Additionally, we employed Linear Discriminant Analysis Effect Size (LEfSe) and Receiver Operating Characteristic (ROC) curve analyses using R packages. For predicting bacterial function, we employed PICRUSt 2 software along with KEGG and METACY databases. Differential analysis was performed using STAMP, and species-related network diagrams were constructed using Gephi 1.0.3.8 software.

2.11. Statistical analysis

We conducted statistical analysis using IBM SPSS Statistics version 24.0 (IBM Corp., Armonk, NY, USA). Continuous data adhering to normality and homogeneity assumptions underwent one-way ANOVA for comparison. Non-parametric tests, such as the Kruskal-Wallis test, were employed for data not meeting these assumptions. Dunnett's multiple comparison test (Tukey test) facilitated inter-group comparisons. Statistical significance was set at $P < 0.05$.

3. Results

3.1. Effects of HXZQS on the symptoms of diarrhea and general behavior in diarrhea mice with CDSS

Our research findings indicate that following successful modeling, model mice exhibited swollen perianal mucosa, redness and slight protrusion around the anus, and thickening of the tail base compared to normal mice. Additionally, they displayed pronounced abdominal wall contractions but experienced difficulty with bowel movements, passing soft or watery stools. The feces were poorly formed and inconsistent in size, accompanied by poor mental state, vacant gaze, and sparse fur.

Upon commencing treatment with HXZQS, mice in the H–Tc group displayed consistent mental states, regular bowel movements, and stools with slight formation on the initial day. However, mice in the H-Mc group still showed signs of agitation, clustering, and drowsiness, with increased abdominal wall contractions and difficulty with bowel movements. By the second day of treatment, mice in the H–Tc group showed restored redness and sensitivity in the perianal and joint mucosa, with improved mobility and smooth bowel movements. Stool color deepened, and stool pellets became uniformly sized and formed. In contrast, mice in the H-Mc group exhibited restored mental states, reduced drowsiness, increased spontaneous activity, and slightly formed stools. By the third day of treatment, mice in the H–Tc group had glossy fur, and their mental states and bowel movements had largely returned to normal. Mice in the H-Mc group showed some improvement, with only slightly disheveled fur and a slightly lethargic demeanor, and looser stool consistency.

As depicted in Table 1, throughout the modeling phase, the diarrhea index notably surged in model mice compared to those in the H-Cc group ($P < 0.01$). Subsequently, during the Chinese medicine intervention period, mice in the H-Mc group exhibited a significant rise in the diarrhea index relative to the H-Cc group ($P < 0.05$), whereas the H–Tc group demonstrated a pronounced reduction in this index compared to the H-Mc group ($P < 0.05$).

3.2. Effects of HXZQS on intestinal digestive enzymes in diarrhea mice with CDSS

During the experiment, we observed that mice exposed to cold and humid environments had wet and soft feces, increased stool frequency, and showed signs of malaise and messy hair, compared to the H-Cc group. However, these symptoms were alleviated after treatment with HXZQS. Fig. 2 illustrates the level of intestinal digestive enzymes in each group. As shown in Fig. 2A–E, in comparison to the H-Mc group, the H–Tc group demonstrated significantly decreased lactase activity in intestinal contents ($P < 0.05$) and slightly lower sucrase activity ($P > 0.05$), which subsequently normalized. Conversely, the H–Tc group exhibited elevated levels of protease, amylase, and cellulase activity in intestinal contents, also returning to normal levels ($P > 0.05$). Moreover, as shown in Fig. 2F–I, the H–Tc group displayed higher levels of intestinal mucosal lactase, mucosal sucrase, and cellulase activity compared to the H-Mc group ($P > 0.05$). However, no significant difference was observed in intestinal mucosal protease activity between the two groups ($P > 0.05$).

3.3. Impact of HXZQS on intestinal microbiota diversities in diarrhea mice with CDSS

The dilution curve analysis (Fig. 3A) indicated that sequencing data volume was sufficient for subsequent analysis. In total, 13, 5158 high-quality bacterial 16S rRNA sequences were acquired, distributed as follows: 4052 sequences in the H-Cc group, 4,3606 in the H-Mc group, and 4,7500 in the H–Tc group. As illustrated in Fig. 3B–a total of 72 OTUs were shared among all three groups. Additionally, unique OTUs were identified: the H-Cc group had 43, the H-Mc group had 52, and the H–Tc group had 61. Fig. 3C showed minimal variation in α diversity across the three groups, suggesting a gradual recovery of species abundance, evenness, and diversity in the intestinal microbiota of the H-Mc and H–Tc groups over time. However, Fig. 3D and E indicated significant differences in the H–Tc group compared to the others, highlighting the substantial impact of HXZQS intervention on the mice's intestinal microbiota composition.

Table 1
Comparison of diarrhea index among three groups of mice ($\bar{x} \pm s$, n = 10) .

Group		The H-Cc group	The H-Mc group	The H–Tc group	*F*	*P*
Modeling Stage	Day 1	0.093 ± 0.001	0.332 ± 0.013##	0.385 ± 0.017	11.83	0.004
	Day 2	0.073 ± 0.001	0.526 ± 0.035##	0.640 ± 0.048	16.69	0.0014
	Day 3	0.166 ± 0.009	1.294 ± 0.362##	1.245 ± 0.194	15.74	0.0017
	Day 4	0.156 ± 0.004	2.880 ± 0.162##	1.667 ± 0.347 **	77.94	< 0.001
	Day 5	0.087 ± 0.001	2.418 ± 0.522##	2.348 ± 0.653	30.58	< 0.001
	Day 6	0.074 ± 0.001	1.143 ± 0.163##	1.600 ± 0.133	29.5	< 0.001
	Day 7	0.040 ± 0.001	1.524 ± 0.121##	1.587 ± 0.104	42.24	< 0.001
Treatment Stage	Day 1	0.120 ± 0.002	1.015 ± 0.043##	0.533 ± 0.036 **	51.61	< 0.001
	Day 2	0.067 ± 0.001	0.790 ± 0.026##	0.200 ± 0.005 **	55.95	< 0.001
	Day 3	0.044 ± 0.041	0.343 ± 0.015##	0.123 ± 0.002 **	20.9	< 0.001

Note: # denotes a significant difference from the H-Cc group (P < 0.05); ## denotes a highly significant difference from the H-Cc group (P < 0.01); * denotes a significant difference from the H-Mc group (P < 0.05). The H-Cc group serves as the normal control (n = 10), the H-Mc group corresponds to the CDSS-induced diarrhea group (n = 10), and the H–Tc group represents the HXZSQ treatment (n = 10). Likewise for subsequent groups.

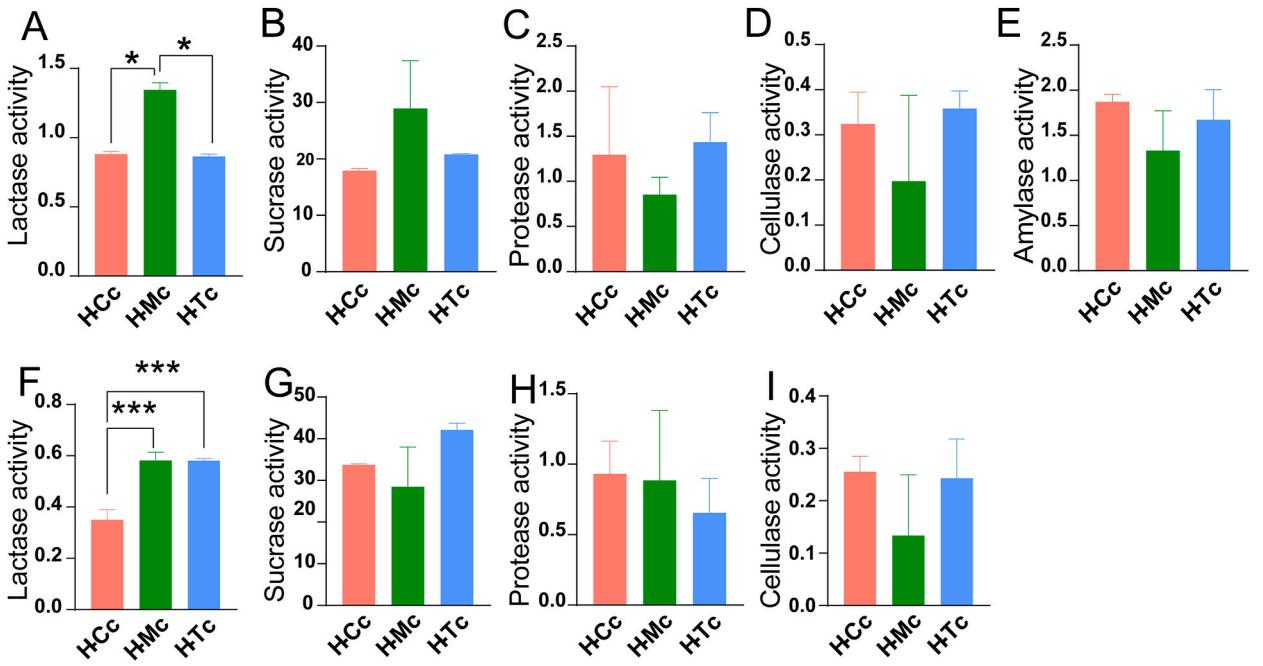

Fig. 2. DEA in intestinal contents and mucosa. A–E: Activities of lactase, sucrase, protease, cellulase, and amylase in intestinal contents, respectively. F–I: Activities of lactase, sucrase, protease, and cellulase in intestinal mucosa, respectively. Data are expressed as mean ± standard deviation (SD). $^{*}P < 0.05$, $^{***}P < 0.001$.

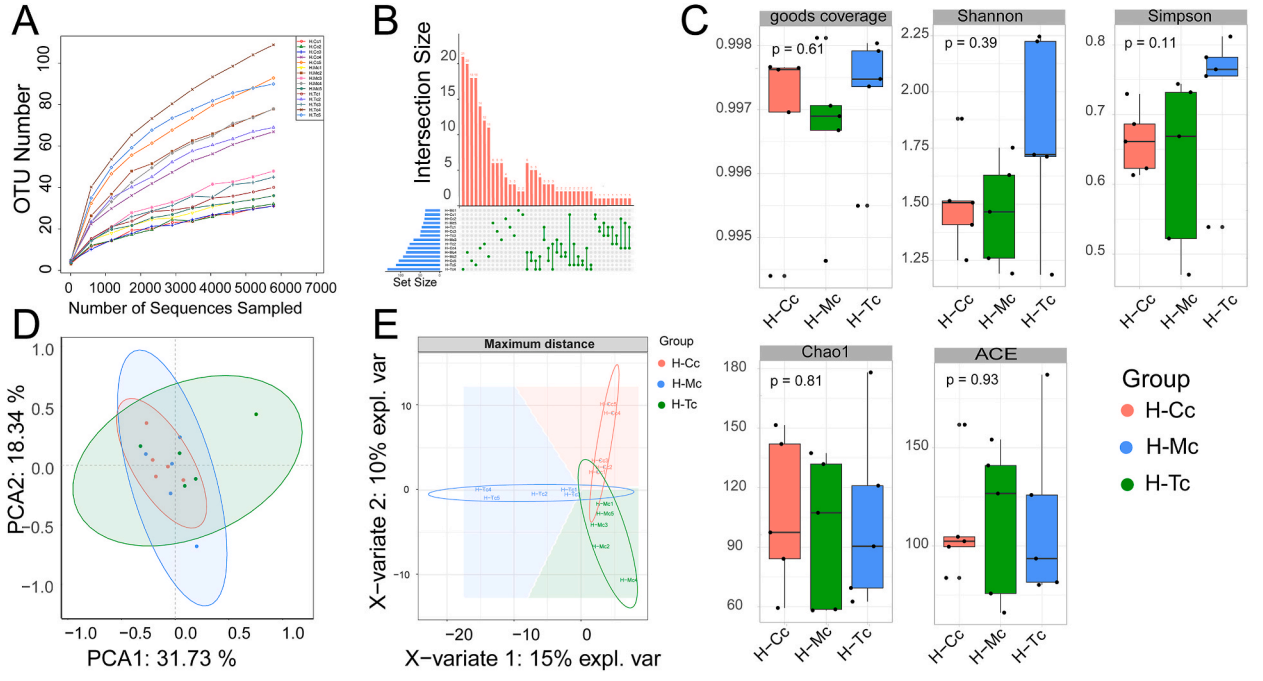

Fig. 3. Diversity and community structure of intestinal microbiota. A: Dilution curve. B: Upset graph. C: Alpha diversity index map, including richness, good coverage, Shannon, Simpson, Chao1, and ACE index. D: Principal component analysis (PCA) graph based on Bray-Curtis distance. E: Partial least squares discriminant analysis (PLS-DA) graph.

3.4. The administration of HXZQS altered the microbial community structure in mice with CDSS

To assess the functions and impacts of microbial taxa, we set thresholds at 1 % for both rare and abundant taxa, organizing all OTUs into separate categories according to their abundance levels. Analysis at the phylum level revealed that three primary groups (Firmicutes, Bacteroidetes, and Proteobacteria) collectively comprised more than 98 % of the microbial community composition (refer to Fig. 4A). Notably, Deferribacteres and Epsilonbacteraeota were absent in the H–Tc group, whereas they continued to exist in the H-Mc group. In Fig. 4B and C, concerning the genus level, *Lactobacillus* and *Candidatus Arthromitus* emerged as the prevailing bacterial genera in both the H-Cc and H–Tc groups, with *Lactobacillus* notably more predominant. The H-Mc group also showed a high abundance of *Lactobacillus* (account for 87.4 %), and a smaller proportion of *Candidatus Arthromitus* (6.26 %) and *Clostridium sensu stricto* 1 (1.97 %). As shown in Fig. 4B and D, at the species level, the H-Cc group was dominated by *Lactobacillus johnsonii* (51.23 %), *Lactobacillus reuteri* (22.27 %), *Lactobacillus murinus* (6.02 %). The H–Tc group was dominated by *Lactobacillus johnsonii* (36.28 %), *Lactobacillus reuteri* (25.37 %), *Lactobacillus murinus* (6.7 %). In contrast, the H-Mc group was dominated by *Lactobacillus johnsonii* (43.53 %), *Lactobacillus murinus* (21.60 %), *Lactobacillus reuteri* (17.17 %) and *Clostridium* sp. ND2 (1.70 %). Notably, the relative abundance of *Clostridium* sp. ND2 exhibited a significant increase in the H-Mc group compared to both the H-Cc and H–Tc groups ($P < 0.05$).

3.5. Differential analysis of intestinal microbiota in diarrhea mice with CDSS intervened by HXZQS

In Fig. 5A, employing LEfSe analysis with LDA scores exceeding 2, we identified *Corynebacterium* and *Clostridiales vadinBB60 group* as differential bacteria in the H–Tc group, while Cyanobacteria unidentified specie was identified as a differential bacterium in the H-Mc group. The ROC curve shown in Fig. 5B demonstrates that *Clostridiales vadinBB60 group*, Cyanobacteria unidentified specie, and *Corynebacterium* exhibit high sensitivity and specificity in distinguishing each group. In discriminating between the H-Mc and H-Cc groups, Cyanobacteria unidentified species demonstrated the highest efficacy, achieving an AUC of 1. Meanwhile, in distinguishing the H-Mc group from the H–Tc group, Cyanobacteria unidentified species and *Corynebacterium* emerged as the most effective, with respective AUC values of 0.74 and 0.8.

3.6. Bacterial gene function prediction in diarrhea mice with CDSS intervened by HXZQS

From Fig. 6A, it is evident that HXZQS had a significant impact on several metabolic functions in mice with cold and humid stress-induced diarrhea, including cofactors and vitamins metabolism, energy metabolism, carbohydrate metabolism, and amino acid metabolism. Fig. 6B indicated that the H–Tc group was effective in restoring and improving metabolic pathways related to terpenoids and polyketides metabolism, cofactors and vitamins metabolism, energy metabolism, and amino acid metabolism, while also reducing functions of carbohydrate metabolism, membrane transport, infectious disease: bacterial, etc. Fig. 6D indicated that C5-Branched dibasic acid metabolism, Lipoarabinomannan biosynthesis, and Biosynthesis of secondary metabolites-unclassified had significant

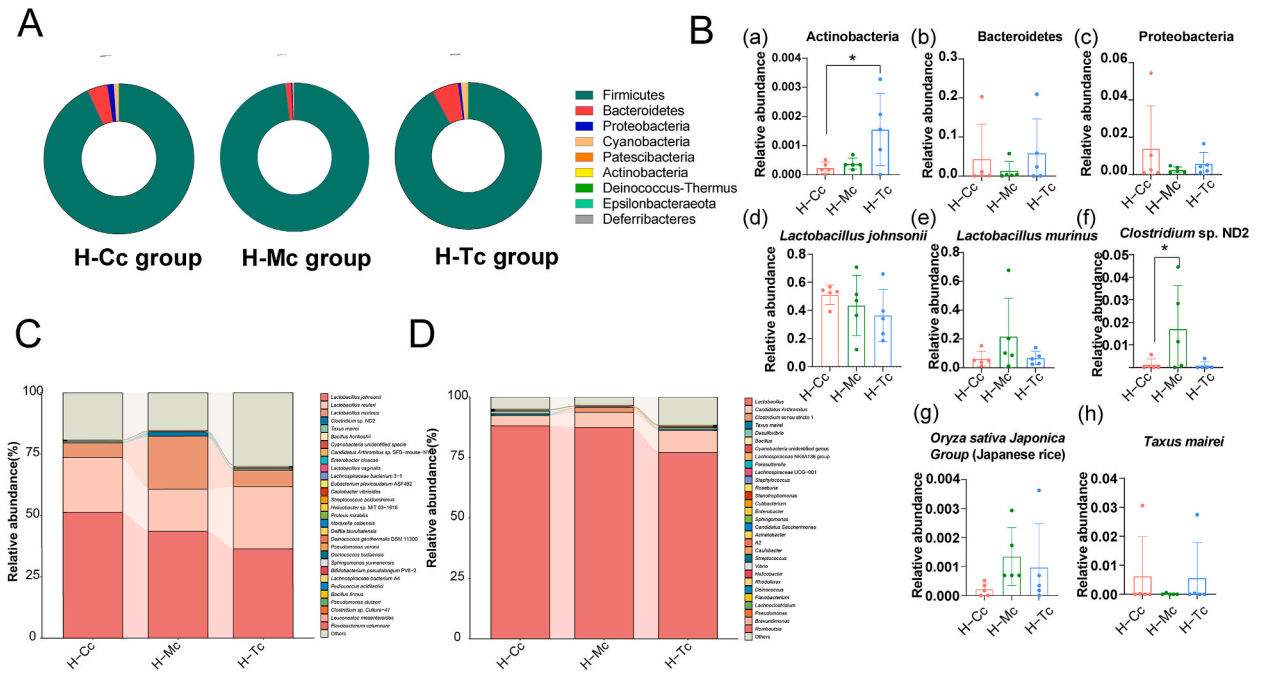

Fig. 4. Species distribution of intestinal microbiota. A: Species distribution and relative abundance at the phylum level. B: Species with significant changes in relative abundance. C and D: Relative abundance at the genus and species levels, respectively. *$P < 0.05$.

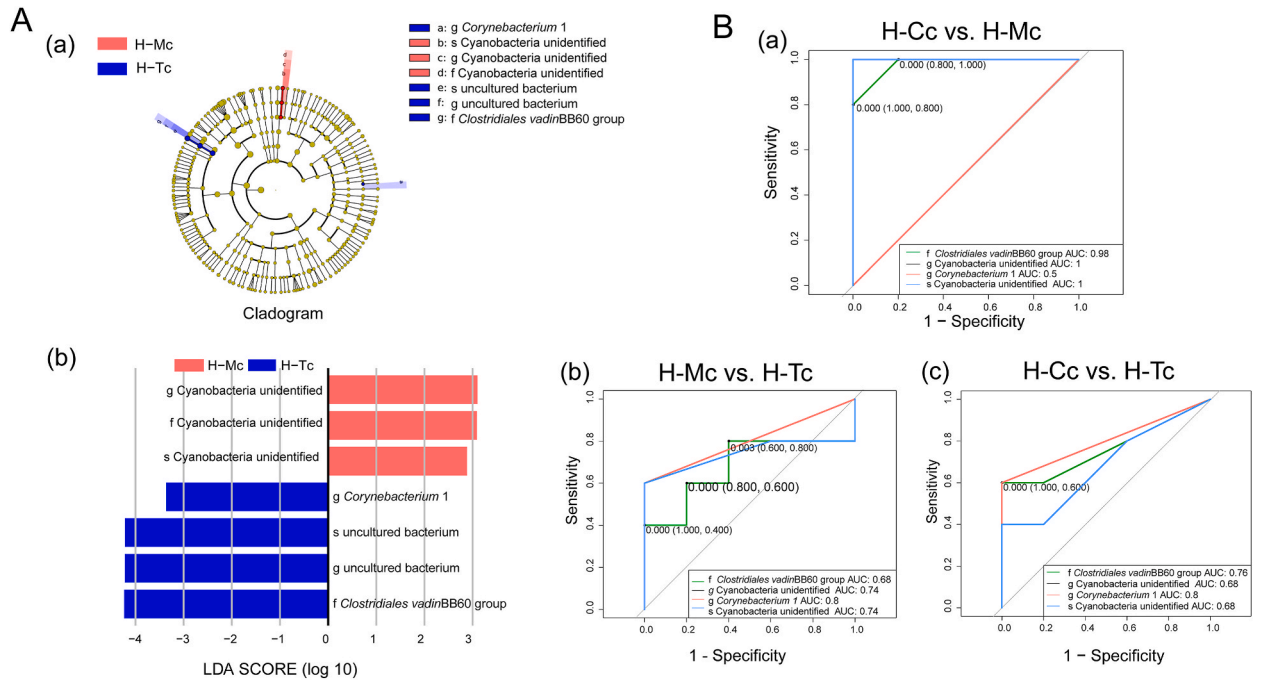

Fig. 5. Analysis of differential bacterial species in the intestinal microbiota. A: LEfSe analysis. B: ROC curve.An AUC value of 1.0 indicates flawless discrimination between the two groups, with no prediction errors. The closer the AUC value is to 1.0, the higher the accuracy of the prediction. AUC values between 0.5 and 0.7 suggest low accuracy, while those between 0.7 and 0.9 indicate reasonable accuracy, and values above 0.9 signify high accuracy. An AUC of 0.5 suggests the diagnostic method is ineffective and lacks diagnostic value. AUC <0.5 rarely occurs in practice and does not reflect the real situation.

differences among the three groups ($P < 0.05$ or $P < 0.01$). The results in Fig. 6C and E demonstrate the impact of HXZQS on the activity of intestinal microbiota metabolic enzymes. For example, L-fucose isomerase (EC:5.3.1.25) activity was altered, resulting in the production of L-fucose, known for its health benefits such as immune enhancement and anti-tumor effects [35]. Similarly, the activity of diacetyl reductase (EC:1.1.1.303) and (R, R)-butanediol dehydrogenase (EC:1.1.1.4), typically associated with butanediol dehydrogenase function, was affected. These enzymes play a role in butyrate metabolism and have been reported to be produced by Saccharomyces cerevisiae [36]. Additionally, enzymes like Inositol 2-dehydrogenase (EC:1.1.1.18), D-chiro-inositol 1-dehydrogenase (EC:1.1.1.369), and sn-glycerol-1-phosphate dehydrogenase (EC:1.1.1.261) underwent changes, influencing processes such as cell growth, energy provision, and cellular repair.

3.7. The shifts in the cooperative patterns of intestinal microbiota in diarrhea mice with CDSS intervention using HXZQS

As demonstrated in Fig. 7A and C, consistent with previous research by our group, modeling led to a competitive and inhibitory relationship between the intestinal probiotics *Lactobacillus johnsonii*, *Lactobacillus reuteri*, and *Lactobacillus murinus*. However, after treatment with HXZQS, the inhibitory competition between them disappeared (Fig. 7B and C). The same change occurred in rare bacteria, and HXZQS restored the original cooperative mode between rare bacteria by slowing down their intensive mutual promotion.

4. Discussion and conclusion

4.1. HXZQS improves the intestinal microbiota of diarrhea mice with CDSS

The findings regarding species abundance revealed that HXZQS primarily elevated and reinstated the presence of *Lactobacillus reuteri* while reducing the population of *Lactobacillus murinus*. It has been reported that an excessive proliferation of *Lactobacillus murinus* due to antibiotic usage can disrupt intestinal metabolic function, leading to conditions such as alopecia in mice [37]. However, *Lactobacillus murinus* has also been reported to prevent intestinal damage [38]. Under energy-restricted conditions, *Lactobacillus murinus* grows rapidly and contributes to maintaining intestinal barrier function, reducing serum endotoxin load, and improving systemic inflammation [39]. *Lactobacillus reuteri*, recognized as a beneficial bacterium, enhances intestinal microbiota and counters the colonization of harmful bacteria. Additionally, it inhibits intestinal inflammatory factors and bolsters intestinal immune function [37, 40–42].

In addition, HXZQS also reduced the abundance of *Clostridium* sp. ND2, a Gram-positive obligate anaerobic of Firmicutes that ferments D-glucose and D-maltose, producing butyric acid [43]. The LEfSe analysis results revealed several differential bacteria among

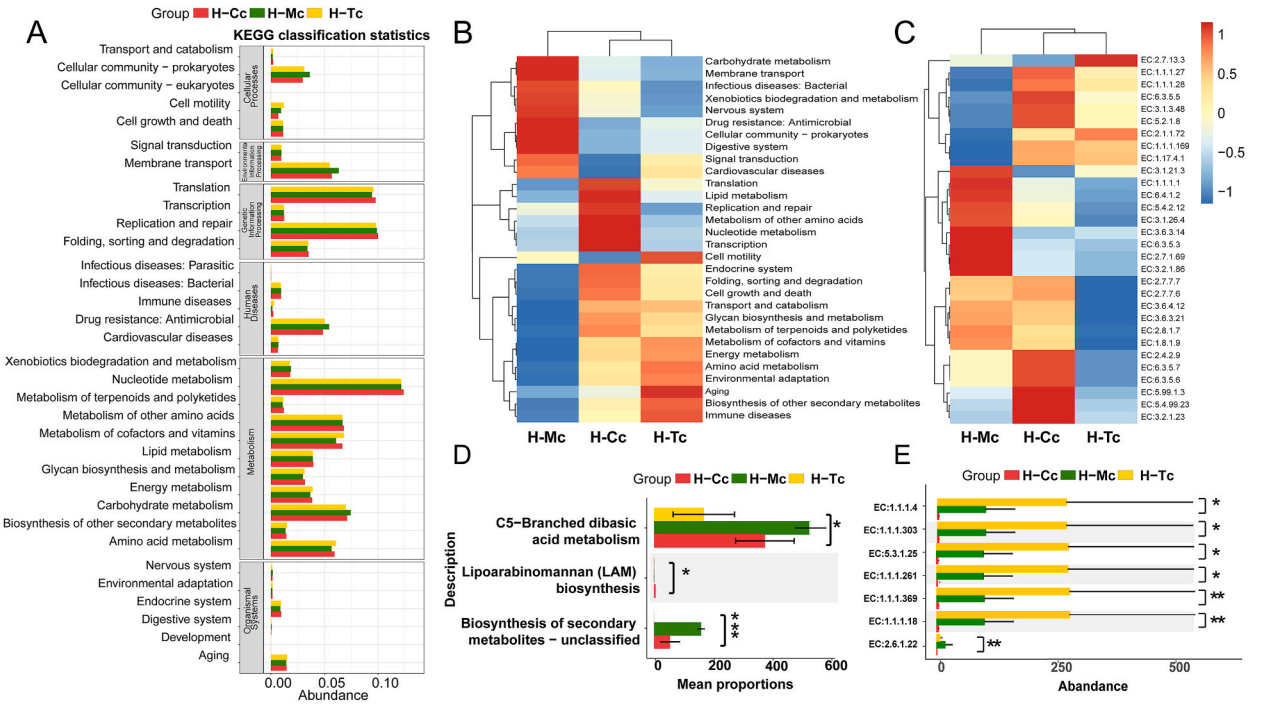

Fig. 6. Analysis of Intestinal Bacterial Functional Prediction. A: Predicted abundance map of KEGG secondary functions. Colors represent group names, the x-axis represents relative abundance, the y-axis represents KEGG secondary functional classification, and titles in gray areas represent corresponding first-level classification names. B: Heatmap displaying the top 30 tertiary function abundances. Horizontal direction represents group names, vertical direction represents function information, the left side displays clustering tree of functions based on relative abundance, and the upper part indicates sample clustering tree. Colors in the heatmap represent relative abundance of functions, where Z values obtained after normalization processing. Closer to red indicates higher abundance. C: Relative abundance of enzymatic functions. D and E: STAMP differential analysis (ANOVA method) based on relative abundance of pathways and enzymes, respectively.*$P < 0.05$, **$P < 0.01$, ***$P < 0.001$. (For interpretation of the references to color in this figure legend, the reader is referred to the Web version of this article.)

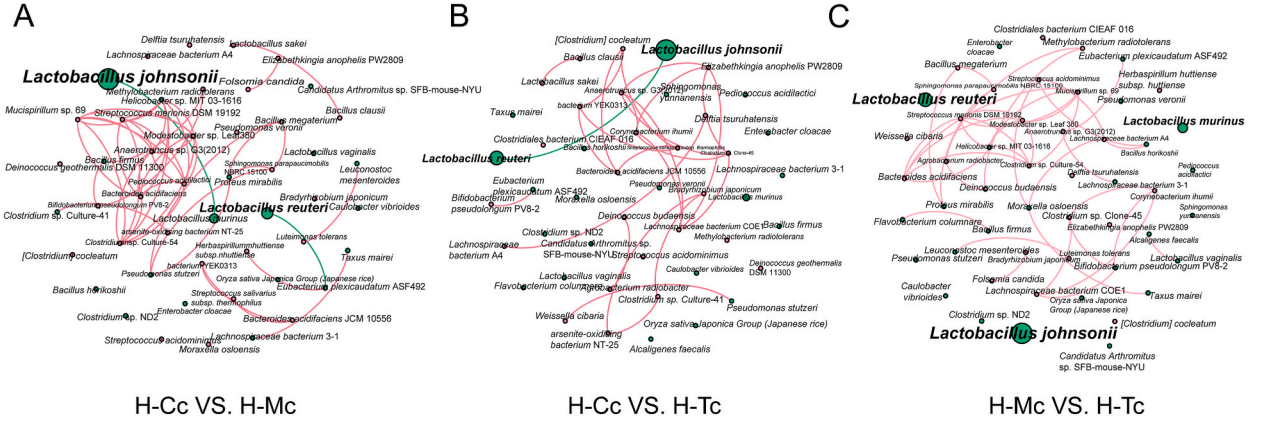

Fig. 7. Intestinal microbiota interaction network. A: Network depicting interactions between rare and abundant species in the intestines of the H-Cc and H-Mc groups. B: Network illustrating interactions between rare and abundant species in the intestines of the H-Cc and H–Tc groups. C: Network showing interactions between rare and abundant species in the intestines of the H-Mc and H–Tc groups. Red nodes denote the presence of rare species, while green nodes signify abundant species; node size is proportional to their respective weights. Correlations between species are depicted by edges: red lines denote positive correlations, while green lines indicate negative correlations. The thickness of the lines corresponds to the strength of the correlation, with connections depicting strong ($r > 0.8$) and statistically significant ($P < 0.05$) correlations. (For interpretation of the references to color in this figure legend, the reader is referred to the Web version of this article.)

the three groups. *Corynebacterium* 1 was diverse and included both pathogenic and nonpathogenic strains. The *Clostridiales* vadin BB60 group, identified as a differential bacterium in the H–Tc group, shows increased abundance under the stimulation of HXZQS decoction. It can produce short-chain fatty acids, which are negatively correlated with obesity, abnormal blood lipids, and insulin resistance, suggesting its potential as a probiotic [44,45].

In line with our prior research, there was an observed increase in Cyanobacteria unidentified specie within the intestinal tract of mice in the H-Mc group, marking them as distinctive bacteria in this group [46]. Notably, HXZQS demonstrates the ability to counteract this phenomenon. Cyanobacteria unidentified specie belonged to the phylum Cyanobacteria, an ancient class of bacteria playing a vital role in biological evolution. Although *Cyanobacteria* can excrete a large amount of C4 dicarboxylic acid through glycogen fermentation in a dark anoxic environment [47], they also produce toxins causing damage to the body [48]. Some studies suggest that Cyanobacteria may be involved in the development of inflammatory bowel diseases such as Crohn's disease and ulcerative colitis, though the exact mechanism remains unclear. Additionally, HXZQS treatment significantly reduced the abundance of an Cyanobacteria unidentified species in the H-Mc group, indicating its potential impact on the intestinal microbiota.

4.2. Effects of HXZQS on intestinal DEA, intestinal microbial abundance and function in diarrhea mice with CDSS

Our research findings indicate that HXZQS significantly decreased lactase activity in intestinal contents and also moderately increases disaccharidase activity, including sucrase and lactase, in the intestinal mucosa. This augmentation contributes to the promotion of intestinal digestive function. We also observed that HXZQS increased the protease activity in the contents of diarrhea mice with CDSS. This is significant, as small intestinal proteases, many of which are microbiota-derived, can negatively impact the immune response to dietary antigens, compromise mucosal barrier integrity, and trigger pro-inflammatory or pro-nociceptive signals [49,50]. The increased protease activity may also be linked to intestinal inflammation and microbiota dysbiosis. Increased protease activity observed in the feces of inflammatory bowel disease (IBD) patients suggests a potential link to gut microbiota dysbiosis in these conditions [51]. Furthermore, HXZQS was found to enhance the activity of intestinal cellulase, which is responsible for breaking down complex carbohydrates such as cellulose. These findings suggest that HXZQS may help improve the digestion and absorption of carbohydrates in diarrhea mice with CDSS. Overall, our study offers valuable insights into the potential benefits of HXZQS in enhancing intestinal DEA, as well as microbial abundance and function, in mice with diarrhea induced by cold and high humidity stress.

In addition to its effects on intestinal digestive enzymes, our study also investigated the impact of HXZQS on intestinal microbial abundance and function in CDSS mice. Our findings suggest that HXZQS inhibited the growth of bacteria such as *Alloprevotella* UCG-001, *Alloprevotella*, *Bacteroides*, *Parabacteroides*, and *Bacteroides acidifaciens*, while increasing the relative abundance of *Marvinbryantia*, a genus known for its ability to decompose cellulose [52]. This is consistent with the observed increase in cellulase activity in intestinal contents in the HXZQS group. Shifts in the predicted function of the intestinal microbiota were aligned with alterations in enzyme activity. Our results showed that HXZQS increased the activity of bacterial amylase, specifically alpha-amylase, which is the most important bacterial amylase accounting for 98.47 % [53]. This was further supported by a rise in the relative presence of crucial amylase-producing bacteria, such as *Bacillus* and *Lactobacillus*, observed in the HXZQS group [54]. Furthermore, our study highlighted the potential negative impact of excessive fermentation of Prevotellaceae and Bacteroidaceae bacteria, which can lead to a reduction in intestinal pH and an imbalance in the intestinal microbiota. HXZQS was found to inhibit the growth of these bacteria, which may contribute to restoring a more balanced intestinal microbiota. Moreover, HXZQS restored the activity of disaccharidases in the small intestinal mucosa while concurrently reducing it in the intestinal contents. This aligns with the decline in relative abundance observed in an unidentified species within the Cyanobacteria phylum, which is recognized for its inhibition of the metabolic process of c-5 branched dibasic acids [55].

This discovery implies that HXZQS could enhance carbohydrate digestion and absorption efficiency within the small intestine, potentially contributing to its overall positive effects on intestinal health. Further investigation is warranted to delve into the underlying mechanisms and potential therapeutic applications of HXZQS concerning intestinal microbial metabolism.

4.3. Regulation of intestinal microbiota interactions by HXZQS improves intestinal health in diarrhea with CDSS

We examined the significance of microbial interactions within the intestine and their connection to microbiota health in cases of diarrhea with CDSS. The microbial ecosystem in the intestinal is a dynamic and complex process, with intricate communication among intestinal microbiota to adapt to the environment [22]. Different interactions such as mutualism, competition, predation/parasitism, favoritism, harmless parasitism, and neutralism shape the stability and dynamics of microbial communities in consortiums. Understanding these microbial interactions can help determine the overall regulation of the intestinal microbiota and targeted regulation of specific bacteria by pharmaceuticals. Network association analysis can be used to study the interaction relationship in the intestinal microbiota under both natural and intervention states [56].

Our study found that when subjected to extreme cold and humid environment stress, intestinal bacteria change the way of cooperation to adapt to the new environment, causing an imbalance in the microbiota and contributing to diarrhea with CDSS. However, we observed that HXZQS can restore the cooperation of the intestinal microbiota, returning it to the state before modeling. HXZQS mainly improved the competition or inhibition strategies of several dominant *Lactobacillus* strains in the intestine while reducing the mutual promotion strategies of the main intestinal rare bacteria. This beneficial change in bacterial interaction can mainly be attributed to the improvement in the distribution of nutrients and energy in the intestinal tract by HXZQS. However, the cooperation among intestinal bacteria is complex, but the molecular mechanism of the ecological relationship between co-cultured

microorganisms is currently poorly understood, and the development of co-culture technology is slow [22,57]. Our findings indicate that HXZQS may be vital in modulating microbiota cooperation and enhancing intestinal microbiome health. Additional research is needed to explore the clinical applications of HXZQS in intestinal microbial metabolism and to uncover the mechanisms behind its beneficial effects.

5. Conclusion

In conclusion, our study sheds light on the therapeutic potential of HXZQS in regulating intestinal lactase activity and restoring microbiota balance in diarrhea with CDSS in mice. HXZQS primarily achieves its therapeutic effects by augmenting the abundance of *Clostridiales vadin*BB60 group while suppressing the proliferation of Cyanobacteria unidentified specie. Moreover, our findings highlight the capacity of HXZQS to reinstate the symbiotic relationship between both rare and abundant bacteria in the gut to pre-modeling levels. Crucially, HXZQS targets and regulates intestinal lactase activity directly, indicating its pivotal role in addressing gastrointestinal disturbances. Furthermore, our observations suggest that HXZQS also impacts the metabolic functions of intestinal bacteria to some degree. This modulation of bacterial metabolism corresponds with observed changes in digestive enzyme activity within the intestine, further underscoring the therapeutic efficacy of HXZQS.

Funding

This research was financially supported by the National Natural Science Foundation of China (Grant Nos. 81874460).

The data availability statement

The data have been deposited at the NCBI database (https://www.ncbi.nlm.nih.gov/) with accession number PRJNA797198.

Ethics approval and consent to participate

All animal experiments were authorized by the Animal Ethics Committee of Hunan University of Chinese Medicine (NO. LL2020102812) and carried out in compliance with the university's guidelines (Changsha, China). Facility use permit number: SYXK (Xiang)2019-0009.

Patient consent for publication

Not applicable.

CRediT authorship contribution statement

Yi Wu: Writing – original draft, Methodology, Formal analysis, Data curation. **Na Deng:** Methodology. **Jing Liu:** Writing – review & editing, Visualization, Methodology. **Ying Cai:** Supervision, Conceptualization. **Xin Yi:** Writing – review & editing, Visualization. **Zhoujin Tan:** Writing – review & editing, Supervision, Funding acquisition, Conceptualization.

Declaration of competing interest

The authors declare that they have no known competing financial interests or personal relationships that could have appeared to influence the work reported in this paper.

Acknowledgements

We gratefully acknowledge the financial support provided by the National Natural Science Foundation of China.

References

[1] Z. Xu, C. Huang, L.R. Turner, H. Su, Z. Qiao, et al., Is diurnal temperature range a risk factor for childhood diarrhea? PLoS One 8 (5) (2013) e64713. https://doi:10.1371/journal.pone.0064713.
[2] H.M. Wu, Z.W. Xu, H.Q. Ao, Y.F. Shi, H.Y. Hu, et al., Differentiation study of Chinese medical syndrome typing for diarrhea-predominant irritable bowel syndrome based on information of four Chinese medical diagnostic methods and brain-gut peptides, Chin. J. Integr. Tradit. West. Med. 35 (10) (2015) 1200–1204. https://doi:10.7661/CJIM.2015.10.1200.
[3] Q.Y. Ye, J.J. Chen, H. Zhou, Q.H. Ling, Q. Wang, et al., Distribution of syndrome types of Chinese medicine in acute infectious diarrhea, Chin. J. Integr. Tradit. West. Med. 36 (6) (2016) 678–680. https://doi:10.7661/CJIM.2016.06.0678.
[4] S.S. Zhang, C.J. Wang, Y.F. Li, N. Wang, Expert consensus on traditional Chinese medicine diagnosis and treatment of diarrhea, Chin. J. Tradit. Chin. Med. 58 (14) (2017) 1256–1260. https://doi:10.13288/j.11-2166/r.2017.14.023.
[5] Y. Su, S. Li, H. Xin, J. Li, X. Li, et al., Proper cold stimulation starting at an earlier age can enhance immunity and improve adaptability to cold stress in broilers, Poultry Sci. 99 (1) (2020) 129–141. https://doi:10.3382/ps/pez570.
[6] Y. Liu, B. Xu, Y. Hu, P. Liu, S. Lian, et al., O-GlcNAc/Akt pathway regulates glucose metabolism and reduces apoptosis in liver of piglets with acute cold stress, Cryobiology 100 (2021) 125–132. https://doi:10.1016/j.cryobiol.2021.02.008.

[7] A.G. Wessels, T. Chalvon-Demersey, J. Zentek, Use of low dosage amino acid blends to prevent stress-related piglet diarrhea, Transl. Anim. Sci. 5 (4) (2021) txab209. https://doi:10.1093/tas/txab209.

[8] D.H. Zhou, G. Liu, The occurrence and evolution of the translation dislocation between the term Pi in traditional Chinese medicine and spleen in western medicine, Stud. Hist. Nat. Sci. 38 (2) (2019) 215–229. http://www.shns.ac.cn/CN/Y2019/V38/I2/215.

[9] H.X. Yuan, X. Huang, Historical evolution of spleen, TCM 7 (6) (2018) 381–390. https://doi:10.12677/TCM.2018.76064.

[10] S.F. Zhou, H.Q. Chen, Y.N. Miao, Analysis of huoxiang Zhengqi san in "taiping huimin hejiju fang", Chin. Folk. Ther. 28 (13) (2020) 9–11. https://doi:10.19621/j.cnki.11-3555/r.2020.1304.

[11] W.X. Du, M.D. Zhu, H.W. Yuan, Dynamic study of correspondence of prescription and syndrome system: a system with combination of disease and syndrome, correspondence of prescription and syndrome, Chin. J. Integr. Tradit. West. Med. 32 (6) (2012) 839–842.

[12] H.J. Zhao, L.P. Guo, F.W. Yang, M.Y. Zhang, L.S. Zhang, et al., Huoxiang Zhengqi formulas for treatment of gastrointestinal type cold: a systematic review and meta-analysis, China J. Chin. Mater. Med. 42 (8) (2017) 1495–1499. https://doi:10.19540/j.cnki.cjcmm.2017.0047.

[13] M. Xiao, J. Tian, Y. Zhou, X. Xu, X. Min, et al., Efficacy of Huoxiang Zhengqi dropping pills and Lianhua Qingwen granules in treatment of COVID-19: a randomized controlled trial, Pharmacol. Res. 161 (2020) 105126. https://doi:10.1016/j.phrs.2020.105126.

[14] M. Xuan, X. Guo, H. Li, T. Xie, X. Mo, et al., The Chinese herbal formula Huoxiang Zhengqi for atopic dermatitis with dampness pattern (CHARM): a study protocol for a double-blinded randomized controlled trial, Trials 22 (1) (2021) 67. https://doi:10.1186/s13063-020-05014-6.

[15] T.L. Lin, C.C. Lu, W.F. Lai, T.S. Wu, J.J. Lu, et al., Role of gut microbiota in identification of novel TCM-derived active metabolites, Protein cell 12 (5) (2021) 394–410. https://doi:10.1007/s13238-020-00784-w.

[16] L. He, C.X. Long, Y.J. Liu, N.Q. Xiao, Z. Tan, J. Regulatory effects of traditional Chinese medicine on the activity of intestinal digestive enzyme, J. Chin. Med. Mater. 40 (8) (2017) 4. https://doi:10.13863/j.issn1001-4454.2017.08.055.

[17] Y.Q. Dong, N. Yang, X.K. Li, S.Y. Chen, W.J. Zhou, et al., Research progress on mechanism of effective components of poorly absorbable oral Chinese materia medica, Chin. Tradit. Herb. Drugs 51 (3) (2020) 769–779. https://doi:10.7501/j.issn.0253-2670.2020.03.030.

[18] Y. Zhao, X. Zhong, J. Yan, C. Sun, X. Zhao, et al., Potential roles of gut microbes in biotransformation of natural products: an overview, Front. Microbiol. 13 (2022) 956378. https://doi:10.3389/fmicb.2022.956378.

[19] Q.L. Shi, Study on Absorption Ingredients of Huoxiang Zhengqi Pill and its Computational Pharmacological Studies on Functional Dyspepsia, Tianjin University, 2014.

[20] T. Wilmanski, N. Rappaport, C. Diener, S.M. Gibbons, N.D. Price, From taxonomy to metabolic output: what factors define gut microbiome health? Gut Microb. 13 (1) (2021) 1–20. https://doi:10.1080/19490976.2021.1907270.

[21] C. Duvallet, S.M. Gibbons, T. Gurry, R.A. Irizarry, E.J. Alm, Meta-analysis of gut microbiome studies identifies disease-specific and shared responses, Nat. Commun. 8 (1) (2017) 1784. https://doi:10.1038/s41467-017-01973-8.

[22] S. Rakoff-Nahoum, K.R. Foster, L.E. Comstock, The evolution of cooperation within the gut microbiota, Nature 533 (7602) (2016) 255–259. https://doi:10.1038/nature17626.

[23] K. Guo, Y. Yan, C. Zeng, L. Shen, Y. He, et al., Study on Baohe pills regulating intestinal microecology and treating diarrhea of high-fat and high-protein diet mice, BioMed Res. Int. (2022) 6891179. https://doi:10.1155/2022/6891179.

[24] C. Long, L. He, Y. Guo, Y. Liu, N. Xiao, et al., Diversity of bacterial lactase genes in the intestinal contents of mice with antibiotic-induced diarrhea, World J. Gastroenterol. 23 (42) (2017) 7584–7593. https://doi:10.3748/wjg.v23.i42.7584.

[25] K. Zhou, M. Peng, N. Deng, Z. Tan, N. Xiao, Lactase bacteria in intestinal mucosa are associated with diarrhea caused by high-fat and high-protein diet, BMC Microbiol. 22 (1) (2022) 226. https://doi:10.1186/s12866-022-02647-2.

[26] V.F. Zevallos, V. Raker, S. Tenzer, C. Jimenez-Calvente, M. Ashfaq-Khan, et al., Nutritional wheat amylase-trypsin inhibitors promote intestinal inflammation via activation of myeloid cells, Gastroenterology 152 (5) (2017) 1100–1113.e12. https://doi:10.1053/j.gastro.2016.12.006.

[27] H. Wang, S. Li, S. Fang, X. Yang, J. Feng, Betaine improves intestinal functions by enhancing digestive enzymes, ameliorating intestinal morphology, and enriching intestinal microbiota in high-salt stressed rats, Nutrients 10 (7) (2018) 907. https://doi:10.3390/nu10070907.

[28] C. Zhang, X. Peng, Y. Wu, M. Peng, T. Liu, et al., Intestinal mucosal microbiota mediate amino acid metabolism involved in the gastrointestinal adaptability to cold and humid environmental stress in mice, Microb. Cell Factories 23 (1) (2024) 33. https://doi:10.1186/s12934-024-02307-2.

[29] J. Li, Pharmacology. Beijing: China Press of Traditional Chinese Medicine, (Ninth Edition), 2016.

[30] J. Zhu, S. Liu, Y. Guo, L. Hou, X. Su, Y. Li, et al., A new model of diarrhea with spleen-kidney yang deficiency dyndrome, Evid. Based Complement. Alternat. Med. (2018) 4280343. https://doi:10.1155/2018/4280343.

[31] M. Zhou, X. Li, J. Liu, Y. Wu, Z. Tan, et al., Adenine's impact on mice's gut and kidney varies with the dosage administered and relates to intestinal microorganisms and enzyme activities, 3 Biotech 14 (3) (2024) 88. https://doi:10.1007/s13205-024-03959-y.

[32] A. Chao, Nonparametric estimation of the number of classes in a population, Scand. J. Stat. 11 (1984) 265–270.

[33] C.E. Shannon, A mathematical theory of communication, Bell Syst. Tech. J. 27 (1948) 379–423. https://doi:10.1002/j.1538-7305.1948.tb01338.x.

[34] E.H. Simpson, Measurement of diversity, Nature 163 (1949) 688. https://doi:10.1038/163688a0.

[35] Y. Huang, H.L. Zhang, Z.L. Li, T. Du, Y.H. Chen, et al., L-fucose, a sugary regulator of antitumor immunity and immunotherapies, Mol. Carcinog. 61 (5) (2022) 439–453. https://doi:10.1002/mc.23394.

[36] J. Heidlas, R. Tressl, Purification and characterization of a (R)-2,3-butanediol dehydrogenase from Saccharomyces cerevisiae, Arch. Microbiol. 154 (3) (1990) 267–273. https://doi:10.1007/BF00248966.

[37] A. Hayashi, Y. Mikami, K. Miyamoto, N. Kamada, T. Sato, et al., Intestinal dysbiosis and biotin deprivation induce alopecia through overgrowth of *Lactobacillus murinus* in Mice, Cell Rep. 20 (7) (2017) 1513–1524. https://doi:10.1016/j.celrep.2017.07.057.

[38] J. Hu, F. Deng, B. Zhao, Z. Lin, Q. Sun, et al., *Lactobacillus murinus* alleviate intestinal ischemia/reperfusion injury through promoting the release of interleukin-10 from M2 macrophages via Toll-like receptor 2 signaling, Microbiome 10 (1) (2022) 38. https://doi:10.1186/s40168-022-01227-w.

[39] F. Pan, L. Zhang, M. Li, Y. Hu, B. Zeng, et al., Predominant gut *Lactobacillus murinus* strain mediates anti-inflammaging effects in calorie-restricted mice, Microbiome 6 (1) (2018) 54. https://doi:10.1186/s40168-018-0440-5.

[40] H. Luo, P. Li, H. Wang, S. Roos, B. Ji, et al., Genome-scale insights into the metabolic versatility of *Limosilactobacillus reuteri*, BMC Biotechnol. 21 (1) (2021) 46. https://doi:10.1186/s12896-021-00702-w.

[41] K. Huang, W. Shi, B. Yang, J. Wang, The probiotic and immunomodulation effects of *Limosilactobacillus reuteri* RGW1 isolated from calf feces, Front. Cell. Infect. Microbiol. 12 (2022) 1086861. https://doi:10.3389/fcimb.2022.1086861.

[42] Z. Yang, A. Wen, L. Qin, Y. Zhu, Effect of coix seed extracts on growth and metabolism of *Limosilactobacillus reuteri*, Foods 11 (2) (2022) 302. https://doi:10.3390/foods11020187.

[43] N. Dione, C.I. Lo, D. Raoult, F. Fenollar, P.E. Fournier, Clostridium massiliamazoniense sp. nov., new bacterial species isolated from stool sample of a volunteer Brazilian, Curr. Microbiol. 77 (9) (2020) 2008–2015. https://doi:10.1007/s00284-020-02099-9.

[44] E. Sawicka-Smiarowska, K. Bondarczuk, W. Bauer, M. Niemira, A. Szalkowska, et al., Gut microbiome in chronic coronary syndrome patients, J. Clin. Med. 10 (21) (2021) 5074. https://doi:10.3390/jcm10215074.

[45] Z. Gao, J. Yin, J. Zhang, R.E. Ward, R.J. Martin, et al., Butyrate improves insulin sensitivity and increases energy expenditure in mice, Diabetes 58 (7) (2009) 1509–1517. https://doi:10.2337/db08-1637.

[46] Y. Wu, N. Deng, J. Liu, P. Jiang, Z. Tan, Alterations in intestinal microbiota and enzyme activities under cold-humid stress: implications for diarrhea in cold-dampness trapped spleen syndrome, Front. Microbiol. 14 (2023) 1288430. https://doi:10.3389/fmicb.2023.1288430.

[47] K. Xu, P. Juneau, Different physiological and photosynthetic responses of three cyanobacterial strains to light and zinc, Aquat. Toxicol. 170 (2016) 251–258. https://doi:10.1016/j.aquatox.2015.11.015.

[48] L.A. Pearson, E. Dittmann, R. Mazmouz, S.E. Ongley, P.M. D'Agostino, et al., The genetics, biosynthesis and regulation of toxic specialized metabolites of cyanobacteria, Harmful Algae 54 (2016) 98–111. https://doi:10.1016/j.hal.2015.11.002.

[49] G. Pontarollo, A. Mann, I. Brandão, F. Malinarich, M. Schöpf, et al., Protease-activated receptor signaling in intestinal permeability regulation, FEBS J. 287 (4) (2020) 645–658. https://doi:10.1111/febs.15055.
[50] A. Caminero, M. Guzman, J. Libertucci, A.E. Lomax, The emerging roles of bacterial proteases in intestinal diseases, Gut Microb. 15 (1) (2023) 2181922. https://doi:10.1080/19490976.2023.2181922.
[51] I.M. Carroll, N. Maharshak, Enteric bacterial proteases in inflammatory bowel disease- pathophysiology and clinical implications, World J. Gastroenterol. 19 (43) (2013) 7531–7543. https://doi:10.3748/wjg.v19.i43.7531.
[52] A. Baniel, K.R. Amato, J.C. Beehner, T.J. Bergman, A. Mercer, et al., Seasonal shifts in the gut microbiome indicate plastic responses to diet in wild geladas, Microbiome 9 (1) (2021) 26. https://doi:10.1186/s40168-020-00977-9.
[53] S. Yan, G. Wu, Analysis on evolutionary relationship of amylases from archaea, bacteria and eukaryota, World J. Microbiol. Biotechnol. 32 (2) (2016) 24. https://doi:10.1007/s11274-015-1979-y.
[54] K. Inan Bektas, A. Nalcaoğlu, E. Ceylan, D.N. Colak, P. Caglar, et al., Isolation and characterization of detergent-compatible amylase-, protease-, lipase-, and cellulase-producing bacteria. Braz. J, Microbiol. 54 (2) (2023) 725–737. https://doi:10.1007/s42770-023-00944-0.
[55] K. Xu, P. Juneau, Different physiological and photosynthetic responses of three cyanobacterial strains to light and zinc, Aquat. Toxicol. 170 (2016) 251–258. https://doi:10.1016/j.aquatox.2015.11.015.
[56] K.Z. Coyte, S. Rakoff-Nahoum, Understanding competition and cooperation within the mammalian gut ,microbiome, Curr. Biol. 29 (11) (2019) R538–R544. https://doi:10.1016/j.cub.2019.04.017.
[57] N.J. Treloar, A. Fedorec, B. Ingalls, C.P. Barnes, Deep reinforcement learning for the control of microbial co-cultures in bioreactors, PLoS Comput. Biol. 16 (4) (2020) e1007783. https://doi:10.1371/journal.pcbi.1007783.